Published by Institute of Physics Publishing for SISSA/ISAS
Received: *March 1, 2002*
Accepted: *March 8, 2002*

Accounting for coherence in interjet E_t flow: a case study

Mrinal Dasgupta
DESY, Theory Group
Notkestrasse 85, Hamburg, Germany
E-mail: dasgupta@mail.desy.de

Gavin P. Salam
LPTHE, Universités P. & M. Curie (Paris VI) et Denis Diderot (Paris VII)
Paris, France
E-mail: salam@lpthe.jussieu.fr

Abstract: Recently, interest has developed in the distribution of interjet energy flows, with for example the leading-log calculation of the highly non-trivial colour structure of primary emissions in 4-jet systems. Here we point out however that at leading-log level it is insufficient to consider only multiple primary emission from the underlying hard antenna — additionally, one must take into account the coherent structure of emission from arbitrarily complicated ensembles of large-angle soft gluons. Similar considerations apply to certain definitions of rapidity gaps based on energy flow. We examine this new class of terms in the simpler context of 2-jet events, and discover features that point at novel aspects of the QCD dynamics.

Keywords: QCD, NLO Computations, Jets, Hadronic Colliders.

JHEP03(2002)017

Contents

1. Introduction

The study of interjet transverse energy (E_t) flow away from jets was suggested by Marchesini & Webber [1] as a method of separating QCD Bremsstrahlung contributions from those of the underlying event in hadron-hadron collisions. Recently, in the $2 + 2$-jet case their considerations on mean energy flows into specified detector regions have been extended by Berger, Kúcs and Sterman [2] to energy-flow *distributions*.

This work apart from its potential phenomenological value at hadron collider experiments also represents theoretical advances in understanding and computing the complex colour topology dictating the flow of soft gluons in 4 jet events, and follows in part from earlier work which discussed perturbative calculations for rapidity gaps in terms of interjet energy flows [3, 4].

One of the main aims of refs. [2, 3, 4] is to resum logarithms L in transverse energy at single-logarithmic accuracy, i.e. all terms $(\alpha_{\rm S} L)^n$. The authors consider the structure of multiple independent soft emissions, and their virtual corrections, from an antenna consisting of the four hard partons (the incoming and outgoing jets) and show how it exponentiates. This is a rather delicate procedure because of the interferences that arise in the colour algebra when squaring the amplitudes involving 4-hard partons and an arbitrary number of soft gluons. The above mentioned studies therefore represent a considerable advance in the field in terms of understanding the 'colour content' of a multi-parton hard scattering (see e.g the discussion in ref. [3]).

In certain contexts, for example for the invariant mass distribution of a dijet pair [5], this exponentiation of what we shall label as *primary* emissions is sufficient. However when considering energy flows in restricted angular regions precisely as in refs. [2], or equivalently definitions of diffraction based on energy cuts [3, 4] (or multiplicity cuts), there is another class of single-logarithmic (SL) terms which must be accounted for. To be more specific it

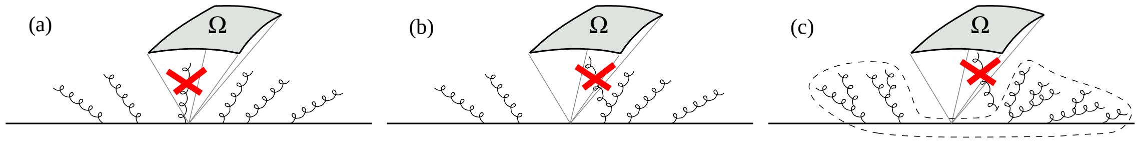

Figure 1: (*a*) veto on primary emissions going into Ω; (*b*) veto on energy-ordered secondary emission going into Ω; (*c*) veto on emissions going into Ω that are radiated coherently from the ensemble made up of all (much) harder emissions not going into Ω.

was shown in ref. [6] that for any observable that is sensitive to radiation in only a part of phase space — a *non-global* observable — it is necessary to account for secondary and higher emissions (as defined below) to obtain an answer correct to SL accuracy.[1]

To illustrate this point better we turn to figure 1, which for simplicity refers to a 2-jet event, though the logic remains the same for the case with several hard jets. It shows a patch Ω in rapidity and azimuth into which the total (transverse) energy flow is restricted to be less than some small amount Q_Ω. There are various sources of SL terms. One source comes from vetoing 'primary' emissions which fly directly into Ω, figure 1a, where primary means that their radiation pattern corresponds to that for the antenna associated with the two hard jets. The lowest-order contribution of this kind comes from an incomplete cancellation between real and virtual terms and gives $-\frac{2\alpha_s C_F}{\pi}\mathcal{A}_\Omega \ln\frac{Q}{Q_\Omega}$, where Q is the hard scale of the problem and $\mathcal{A}_\Omega$ relates to the area of Ω.

A second source of SL terms comes from diagrams such as figure 1*b*. Here we have a large-angle[2] primary emission which flies outside Ω, with energy Q_1, such that $Q \gg Q_1 \gg Q_\Omega$ — this gives us one power of $\alpha_s \ln\frac{Q}{Q_\Omega}$. Forbidding it from radiating a secondary emission into Ω gives powers of $\alpha_s \ln\frac{Q_1}{Q_\Omega}$, which after integration over Q_1 translate into a set of SL terms, $(\alpha_s \ln\frac{Q}{Q_\Omega})^n$. This kind of term has been neglected in [2, 3, 4], as well as in several other contexts [7, 8, 9]. To correctly account for it at all orders it is necessary to consider soft emission into Ω which is *coherently* radiated from arbitrary ensembles of soft (but harder), large-angle energy ordered gluons outside of Ω, figure 1*c*, rather than from just the hard partons in the picture. For simplicity we call this kind of emission a secondary emission, though this is only a figure of speech, since it is coherently radiated from external ensembles which may consist of primary, secondary, tertiary, etc. gluons. In general we refer to the class of terms generated by such contributions as non-global logarithms.

In earlier work [6] we calculated such terms for observables sensitive to radiation in a single hemisphere of a two-jet event. This was done exactly to second order in $\alpha_s \ln\frac{Q}{Q_\Omega}$, and numerically in the large-N_C limit at all orders. Here we extend this work to the case of interjet energy flow in two-jet events. We view this in part as an intermediate step to a calculation in the 3 and 4-jet cases, however it also has value in its own right. Firstly it

[1] Another context in which non-global terms would be relevant is if one were to attempt to carry out a resummation to single-logarithmic accuracy for certain kinds of isolation criteria for isolated photons. However we are not aware of any such resummation being currently in existence.

[2] Strictly speaking, large-angle means of the same order as the angles involved in the definition Ω — if Ω has a boundary at a small angle to a hard-parton axis, then large-angle can actually mean 'of the same order as that small angle.'

JHEP03(2002)017

will turn out that an analysis of the dependence of the effect on the geometry of the patch Ω casts considerable light on the dynamical mechanisms involved in non-global effects. Secondly it allows us to make a general order of magnitude estimate of the importance of non-global terms relative to those from the resummation of primary emissions. Finally the measurement of energy-flow distributions in 2-jet events in e^+e^- collisions or DIS could well be of intrinsic interest since it would be complementary to measurements in hadron-hadron collisions, and in particular, free of the problems associated with the underlying event.

2. Primary emission form factor

In this paper we shall be considering as our observable the amount of transverse energy E_t flowing into a patch Ω in rapidity and azimuth:

$$E_t = \sum_{i\in\Omega} E_{t,i}\,. \tag{2.1}$$

We are interested in the probability Σ_Ω for E_t to be less than some value Q_Ω which is much smaller than the hard scale Q of the process in question:

$$\Sigma_\Omega(Q_\Omega, Q) = \frac{1}{\sigma}\int_0^{Q_\Omega} dE_t\,\frac{d\sigma}{dE_t}\,, \tag{2.2}$$

where σ is the Born-order cross section for the process — in our case the production of two jets in e^+e^- or of $1+1$ jets in DIS.

In order, later on, to quantify the effect of non-global logs it is useful first to calculate the contribution to Σ_Ω from primary emissions alone. This is the much simpler 2-jet analogue of what has been calculated in [2] for 4-jet systems.

At first order in α_{S}, the logarithmically enhanced contribution to Σ_Ω comes from the incomplete cancellation of real and virtual contributions for a soft primary emission:

$$\Sigma_\Omega^{(1)}(Q_\Omega, Q) = -4C_F\frac{\alpha_s}{2\pi}\int_{Q_\Omega}^{Q/2}\frac{dk_t}{k_t}\int_\Omega d\eta\frac{d\phi}{2\pi} = -\frac{4C_F\alpha_{\mathrm{S}}}{2\pi}\mathcal{A}_\Omega\,\ln\frac{Q}{2Q_\Omega}\,, \tag{2.3}$$

where we have introduced the notation $\mathcal{A}_\Omega$ for *area* of the region Ω,

$$\mathcal{A}_\Omega = \int_\Omega d\eta\,\frac{d\phi}{2\pi}\,. \tag{2.4}$$

The upper limit in the k_t integral is arbitrary to single-log accuracy, as long as it is of order Q.

When the logarithm of Q/Q_Ω becomes large enough to compensate the smallness of α_{S}, it is necessary to include terms $(\alpha_{\mathrm{S}}\ln\frac{Q}{Q_\Omega})^n$ to all orders. If one assumes (incorrectly, as we shall see) that multiple wide-angle soft gluons from a two-jet system are simply radiated independently according to a two-particle antenna pattern, then eq. (2.3) can be extended to all orders by accounting for the running of the coupling[3] and then exponentiating the answer:

$$\Sigma_{\Omega,\mathcal{P}}(Q_\Omega, Q) \equiv \Sigma_{\Omega,\mathcal{P}}\left(t(Q_\Omega, Q)\right) = \exp\left[-4C_F\mathcal{A}_\Omega t\right]. \tag{2.5}$$

[3]Strictly speaking the running of the coupling is connected with the collinear branching of the primary gluons. This however is a separate issue from that of large-angle soft gluon emission with which we deal later on in this article.

JHEP03(2002)017

The subscript $\mathcal{P}$ on $\Sigma_{\Omega,\mathcal{P}}$ serves as a reminder that we have only taken into account primary emissions and t is defined to be the following integral of α_s,

$$t(Q_\Omega, Q) = \frac{1}{2\pi}\int_{Q_\Omega}^{Q/2} \frac{dk_t}{k_t}\alpha_s(k_t) = \frac{1}{4\pi\beta_0}\ln\frac{\alpha_s(Q/2)}{\alpha_s(Q_\Omega)}\,, \tag{2.6}$$

where the second equality holds at the one-loop level and $\beta_0 = (11C_A - 2n_f)/(12\pi)$.

3. Leading order calculation of non-global effects

As well as dealing with primary emissions, it is necessary to account also for contributions from (secondary) emissions coherently radiated into Ω from large-angle soft-gluon ensembles outside of Ω. We will denote the contribution from such non-global terms by the function $\mathcal{S}(t)$, such that to SL accuracy

$$\Sigma_\Omega(t(Q_\Omega, Q)) \equiv \mathcal{S}(t)\,\Sigma_{\Omega,\mathcal{P}}(t)\,. \tag{3.1}$$

To start with, we calculate the leading order contribution to $\mathcal{S}$, i.e. $\mathcal{S}_2$, where we define the following series expansion for $\mathcal{S}$:

$$\mathcal{S}(t) = \sum_{n=2}\mathcal{S}_n t^n\,. \tag{3.2}$$

Since this kind of contribution only starts with secondary emissions, there is no $\mathcal{S}_1$ term. In the calculation of $\mathcal{S}_2$, we shall be entitled to equate t with $\frac{\alpha_s}{2\pi}\ln\frac{Q}{2Q_\Omega}$.

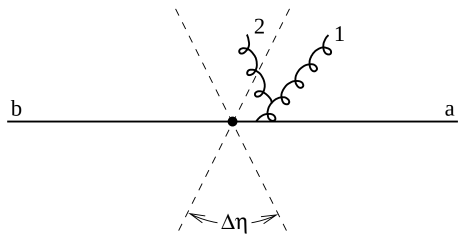

Figure 2: The kind of diagram to be considered for the calculation of $\mathcal{S}_2$ in the case of a rapidity slice of width $\Delta\eta$.

The exact value of $\mathcal{S}_2$ depends on the geometry of the patch Ω. Here we calculate it analytically for the case where Ω is a slice in rapidity of width $\Delta\eta$. The kind of diagram to be considered is shown in figure 2, where a and b are quarks (they may be outgoing or incoming depending on whether for example we are dealing with e^+e^- or DIS in the Breit frame) and 1 and 2 are gluons. We introduce the following four-momenta

$$k_a = \frac{Q}{2}(1,0,0,1)\,, \tag{3.3a}$$

$$k_b = \frac{Q}{2}(1,0,0,-1)\,, \tag{3.3b}$$

$$k_1 = x_1\frac{Q}{2}(1,0,\sin\theta_1,\cos\theta_1)\,, \tag{3.3c}$$

$$k_2 = x_2\frac{Q}{2}(1,\sin\theta_2\sin\phi,\sin\theta_2\cos\phi,\cos\theta_2)\,, \tag{3.3d}$$

where we have defined energy fractions $x_{1,2} \ll 1$ for the two gluons. To our accuracy, we can neglect the recoil of the hard particles against the soft gluons.

We write the squared matrix element for energy-ordered two-gluon emission as (see for example [10])

$$\begin{aligned} W &= 4C_F \frac{(ab)}{(a1)(1b)} \left(\frac{C_A}{2} \frac{(a1)}{(a2)(21)} + \frac{C_A}{2} \frac{(b1)}{(b2)(21)} + \left(C_F - \frac{C_A}{2} \right) \frac{(ab)}{(a2)(2b)} \right) , \\ &= C_F^2 W_1 + C_F C_A W_2 \,, \end{aligned} \tag{3.4}$$

where $(ij) = k_i \cdot k_j$. The result is valid for $1 \gg x_1 \gg x_2$ as well as for the opposite ordering of the gluons, and in addition is completely symmetric under interchange of k_1 and k_2. (We have however chosen to write it in an asymmetric form so as to emphasise the dipole structure of the emissions, namely radiation of gluon k_1 from the ab dipole, followed by the radiation of gluon k_2 from the $a1$, $1b$ and ab dipoles).

The C_F^2 piece of the matrix element, W_1 corresponds to independent gluon emission and is included in the primary emission form factor. To study specifically the modification relative to the primary emission case, at this order one must consider the $C_F C_A$ part of the emission probability, W_2.

For a general region Ω, $\mathcal{S}_2$ is defined through the following equation:

$$\begin{aligned} \mathcal{S}_2 \ln^2 \frac{Q}{2Q_\Omega} + \mathcal{O}\left(\ln \frac{Q}{Q_\Omega} \right) &= -C_F C_A \int_{k_1 \notin \Omega} d\cos\theta_1 \frac{d\phi_1}{2\pi} \int_{k_2 \in \Omega} d\cos\theta_2 \frac{d\phi_2}{2\pi} \times \\ &\times \frac{Q^4}{16} \int_0^1 x_2 dx_2 \int_{x_2}^1 x_1 dx_1 \, \Theta\left(x_2 - \frac{2Q_\Omega}{Q} \right) W_2 \,, \end{aligned} \tag{3.5}$$

which takes into both virtual and real contributions. In the case of a slice of width $\Delta\eta$, the angular integrals can be rewritten explicitly

$$\begin{aligned} &\int_{k_1 \notin \Omega} d\cos\theta_1 \frac{d\phi_1}{2\pi} \int_{k_2 \in \Omega} d\cos\theta_2 \frac{d\phi_2}{2\pi} \to \\ &\qquad \to \left(\int_{-1}^{-c} d\cos\theta_1 + \int_c^1 d\cos\theta_1 \right) \int_{-c}^{c} d\cos\theta_2 \int_0^{2\pi} \frac{d\phi_1}{2\pi} \int_0^{2\pi} \frac{d\phi_2}{2\pi} \,, \end{aligned} \tag{3.6}$$

where we have centred the slice at $\eta = 0$ (the results are independent of its position) and defined $\pm c$ to be the cosines of the polar angles delimiting the slice,

$$\Delta\eta = \ln \frac{1+c}{1-c} \,. \tag{3.7}$$

The integrals over the energy fractions in (3.5) are straightforward. Keeping only the leading-logarithmic piece, exploiting the symmetry in $\theta_1 \leftrightarrow \pi - \theta_1$ and performing the azimuthal average we have

$$\mathcal{S}_2 = -4C_F C_A \int_{-1}^{-c} d\cos\theta_1 \int_{-c}^{c} d\cos\theta_2 \, F_2(\cos\theta_1, \cos\theta_2) \,, \tag{3.8}$$

where the angular function F_2 is

$$F_2 = \frac{2}{(\cos\theta_2 - \cos\theta_1)(1 - \cos\theta_1)(1 + \cos\theta_2)} \,. \tag{3.9}$$

Integrating over the polar angles we obtain

$$\mathcal{S}_2 = -4C_FC_A\left[\frac{\pi^2}{12} + \ln^2\frac{1+c}{1-c} - \ln\frac{1+c}{1-c}\ln\left(\left(\frac{1+c}{1-c}\right)^2 - 1\right) - \right.$$
$$\left. -\frac{1}{2}\mathrm{Li}_2\left(\left(\frac{1-c}{1+c}\right)^2\right) - \frac{1}{2}\mathrm{Li}_2\left(1-\left(\frac{1+c}{1-c}\right)^2\right)\right], \tag{3.10}$$

which can be expressed in terms of $\Delta\eta$ as follows:

$$\mathcal{S}_2 = -4C_FC_A\left[\frac{\pi^2}{12} + (\Delta\eta)^2 - \Delta\eta\ln\left(e^{2\Delta\eta}-1\right) - \frac{1}{2}\mathrm{Li}_2\left(e^{-2\Delta\eta}\right) - \frac{1}{2}\mathrm{Li}_2\left(1-e^{2\Delta\eta}\right)\right], \tag{3.11}$$

where the dilogarithm function is defined as

$$\mathrm{Li}_2(z) = \int_z^0 \frac{\ln(1-t)}{t}dt\,. \tag{3.12}$$

The functional dependence of $\mathcal{S}_2$ on $\Delta\eta$ is shown in figure 3. For small $\Delta\eta$, $\mathcal{S}_2$ goes to zero essentially linearly in η,

$$\mathcal{S}_2 = -4C_FC_A[2(1-\ln 2\Delta\eta)\Delta\eta + \Delta\eta^2 + + \mathcal{O}\left(\Delta\eta^3\right)], \tag{3.13}$$

with a logarithmic enhancement due to the integrable divergence in eq. (3.8) when $\theta_1 \simeq \theta_2 \simeq -c$ — thus $\mathcal{S}_2$ is roughly proportional to the area of the slice. On the other hand as $\Delta\eta$ increases, $\mathcal{S}_2$ rapidly saturates at its asymptotic value,

$$\lim_{\Delta\eta\to\infty}\mathcal{S}_2 = -C_FC_A\frac{2\pi^2}{3}\,. \tag{3.14}$$

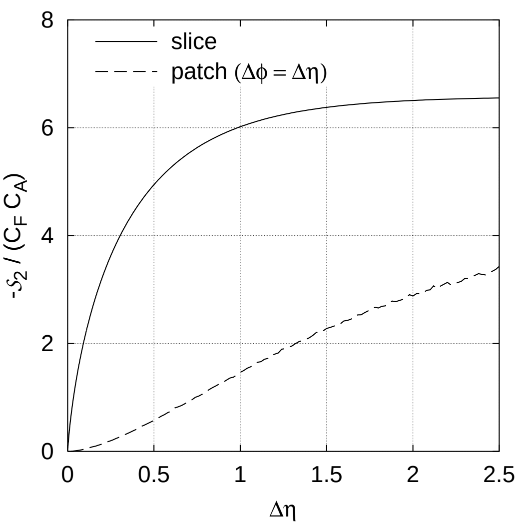

Figure 3: $\mathcal{S}_2$ as a function of $\delta\eta$ for two different definitions of Ω: a slice in rapidity (using eq. (3.11)), and a square patch in rapidity and azimuth with $\delta\phi = \delta\eta$ ($\mathcal{S}_2$ determined numerically).

There is a simple physical reason for this behaviour: $\mathcal{S}_2$ is associated with the difference between full coherent emission for a pair of gluons, and simple independent emission. The dominant contribution to $\mathcal{S}_2$ comes therefore from the region where the two gluons are close together (which by definition means the edges of Ω since one gluon is in, while the other is out). On the other hand, when the two gluons are widely separated in rapidity then independent emission becomes a good approximation and there is no contribution to $\mathcal{S}_2$ — hence for large $\Delta\eta$, $\mathcal{S}_2$ receives no contribution from the centre of the slice, only from its edges, and the value of $\mathcal{S}_2$ saturates.

JHEP03(2002)017

As well as showing $\mathcal{S}_2$ for a slice, figure 3 also shows it (determined numerically) for a square patch in rapidity and azimuth. Over the range of $\Delta\eta = \Delta\phi$ shown, the behaviour is quite different, with an approximate linearity in $\Delta\eta$ — this too can be understood from the above arguments: since it is the edges of Ω which contribute dominantly to $\mathcal{S}_2$, the value of $\mathcal{S}_2$ will be roughly proportional to the perimeter of the patch, and hence linear in $\Delta\eta$. This holds however only for moderate patch sizes: for very small patches, $\mathcal{S}_2$ is roughly proportional to the patch area (with a logarithmic enhancement of similar origin to that for the slice), while for large patches the periodicity in ϕ means that the patch tends to a slice.

4. All-orders treatment

While for the 2-gluon case the analytical calculations are relatively straightforward, in the many-gluon case the situation is vastly more complex: not only does emission into Ω come from a 'Mexican-cactus'-like external multi-gluon ensemble, but the evolution with t of the ensemble outside Ω depends itself on the structure developed at smaller t. Difficulties come from both the geometry and the colour structure of the ensemble. As a result, we have not succeeded in obtaining even approximate analytical results, and we have to resort to the large-N_C approximation and numerical methods in order to extend our calculations to the all-orders case.

4.1 Possible underlying dynamics

Before going on to the details of the numerical results it is however instructive to consider some very rough arguments concerning the underlying dynamics. One way in which Ω can stay empty is simply to prevent all emitters outside of Ω from emitting into Ω. For each emitter 'close' to the edge of Ω the price to pay is roughly e^{-t} (we ignore the coefficient of t); since, to a first approximation, the typical number of relevant emitters will be of order t, we end up with a suppression that goes as e^{-t^2}.

Of course when considering very rare configurations, it is risky to base one's arguments on average properties of the ensemble, such as the typical number of emitters close to the edge. For example, instead of suppressing radiation into Ω from gluons in the neighbourhood of Ω, one could just as well envisage a situation where the neighbourhood of Ω is empty, automatically avoiding secondary emissions into Ω. We shall try to work through this argument with the additional characteristic that we shall discretise the problem. Taking Ω as a slice of width $\Delta\eta$ (sufficiently wide that the two edges can be considered completely independent), the probability of it staying empty down to some scale t is $e^{-4C_F t\Delta\eta}\mathcal{S}(t)$. Let us suppose that the condition for secondary radiation not to be emitted into Ω is determined by the probability that bands of width $\delta\eta$ ('buffers') on either side of the slice stayed empty down to a scale $t - \delta t$. Then we have a recurrence relation:

$$e^{-4C_F t\Delta\eta}\mathcal{S}(t) = e^{-4C_F[t\Delta\eta + 2(t-\delta t)\delta\eta]}\mathcal{S}(t - \delta t)\,, \tag{4.1}$$

where the term proportional to $\delta\eta$ in the exponent stems from the suppression of primary emission in the 'buffer' bands. Rewriting (4.1) as a differential equation, we have

$$\frac{\delta \ln \mathcal{S}}{\delta t} = -8C_F t \left\langle \frac{\delta\eta}{\delta t} \right\rangle . \tag{4.2}$$

The factor $\langle \delta\eta/\delta t \rangle$ can be understood as the average 'speed of motion' (probably proportional to C_A) of the border between regions with and without emissions (i.e. of the edge of the buffer). The resulting form for $\mathcal{S}$ is

$$\mathcal{S}(t) \sim e^{-4C_F t^2 \langle \frac{\delta\eta}{\delta t} \rangle} , \tag{4.3}$$

where we have (arbitrarily) assumed $\langle \delta\eta/\delta t \rangle$ to be independent of t.

One of the features of this mechanism is that resolving only those emissions harder than some intermediate scale t', one will see an extended empty buffer region surrounding Ω, as in figure 4 (shown for one side of a wide slice). The typical size of this buffer region should be of the order of

$$\eta_{\text{buffer}} \simeq (t - t') \left\langle \frac{\delta\eta}{\delta t} \right\rangle . \tag{4.4}$$

It is the suppression of intermediate-scale primary radiation in the buffer region which is responsible for the strong suppression of $\mathcal{S}(t)$ at large t, eq. (4.3).

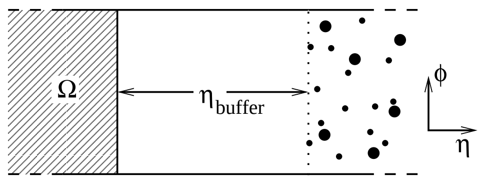

Figure 4: A possible structure for emissions harder than some intermediate resolution scale t' for an event in which Ω stays empty down to some scale $t > t'$. In this scenario, at scale t' an empty buffer region exists between Ω and the emission closest to Ω.

An important consequence of the existence of such a buffer region is that the large-t behaviour of $\mathcal{S}(t)$ would be independent of the shape and size of Ω. This is because at large t the edges of the buffer region will be far from Ω and so the details of Ω can have no influence on the dynamics at the edge of the buffer. This independence on the geometry of Ω, together with the explicit observation of a buffer region, would allow us to distinguish the buffer mechanism from the alternative mechanism proposed at the beginning of this subsection.

4.2 Numerical results

We mentioned above that there are two main problems in obtaining all-order results. One is the complexity of the colour algebra in the presence of large numbers of gluons. This can be eliminated by taking the large-N_C approximation, in which the squared matrix element radiation can be broken down into a sum of independent terms each associated with a different colour dipole [11].

The second source of complexity is the geometry of multi-gluon events, which we treat using a Monte Carlo algorithm like that discussed in [6], which essentially models a tree-like sequence where a colour dipole emits a gluon, thus branching into two dipoles, each of which may themselves go on to emit (there is a similarity to the Ariadne event

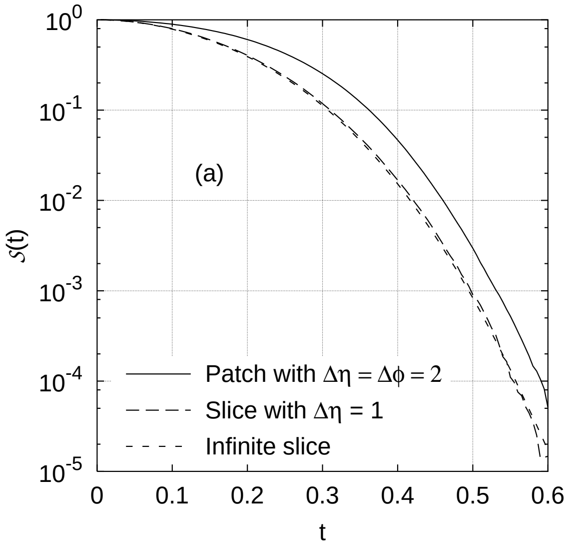

Figure 5: A comparison between (a) the full result for $\mathcal{S}$ and (b) the simple exponentiation of $\mathcal{S}_2$. Beyond $t = 0.5$ the differences between the curves for the finite and infinite slices are not significant compared to the statistical and systematic errors involved in the determination of $\mathcal{S}$.

generator [12]). However unlike a Monte Carlo event generator such as Ariadne, our method has the property that it gives results which are purely a function of t (eq. (2.6)), and therefore contain just the piece which is guaranteed to be correct, namely the leading logarithmic piece.

The Monte Carlo algorithm returns a function $\mathcal{S}_{\rm MC}(t)$ in the large-N_C limit. We choose to correct this function so that at least at order α_s^2 the result is correct beyond the large-N_C approximation. Accordingly, in what follows, we shall consider

$$\mathcal{S}(t) = \left[\mathcal{S}_{\rm MC}(t)\right]^{\frac{2C_F}{C_A}}\,, \tag{4.5}$$

rather than $\mathcal{S}_{\rm MC}$ itself.

In figure 5a we show the function $\mathcal{S}(t)$ for three different geometries for Ω: a square patch in rapidity and azimuth ($\Delta\eta = \Delta\phi = 2$), a finite slice in rapidity ($\Delta\eta = 1$) and an infinite slice in rapidity. We extend the t scale beyond the phenomenologically relevant region in order to better illustrate the general features of $\mathcal{S}$ in the different cases. The right-hand plot, figure 5b shows what would be obtained if there were a simple exponentiation of the $\mathcal{S}_2$ term, $\mathcal{S} \simeq \exp(\mathcal{S}_2 t^2)$.

There are various points to be noted: firstly, as t increases, $\mathcal{S}$ decreases with a behaviour roughly consistent with a Gaussian suppression, at least for $t \lesssim 0.5$. Secondly, at large t, though the normalisation of $\mathcal{S}(t)$ depends on the geometry of Ω, its behaviour in t seems to be *universal.* This is to be compared to the geometry dependence that would be present if the all-orders result stemmed from a simple exponentiation of the $\mathcal{S}_2$ term, figure 5b. We note that up to $t \simeq 0.5$, there is a strong similarity between the actual t-dependence and that observed in the exponentiation of $\mathcal{S}_2$ for an infinite slice. Beyond $t \simeq 0.5$ however the suppression in the full calculation seems to grow much faster.

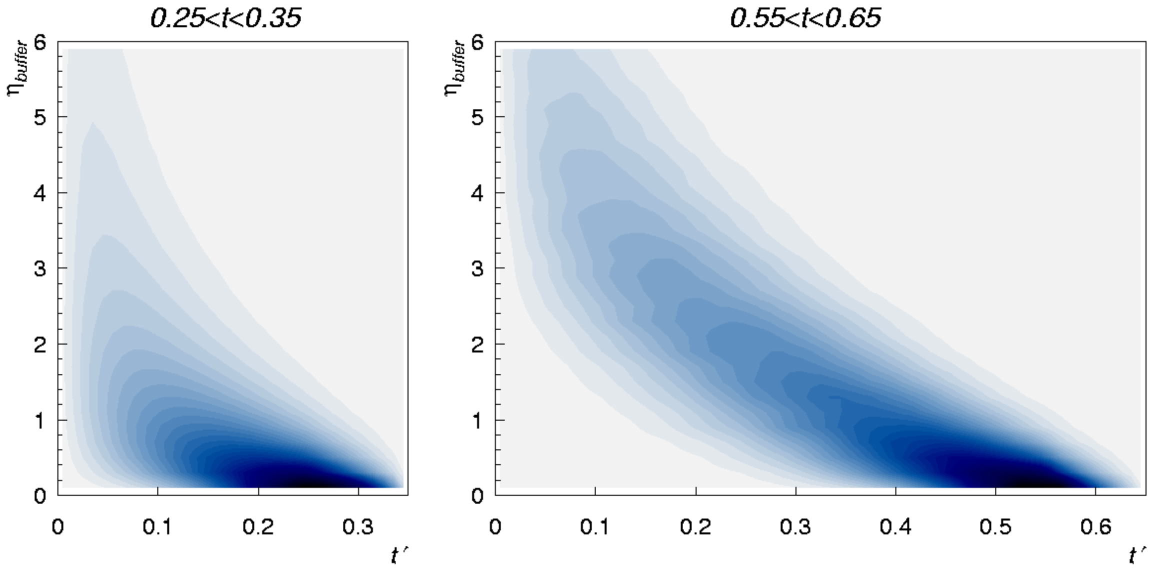

Figure 6: Contour plots for the distribution of the size of the buffer region, $\eta_{\rm buffer}$, as a function of the intermediate resolution scale t'. For the larger t range, the irregularities of the contours are an artifact due to limited statistics. The darkest contour corresponds to $\frac{1}{\sigma}\frac{d\sigma}{d\eta_{\rm buffer}} = 2$.

The fact that the t-dependence of $\mathcal{S}$ is the same regardless of the geometry of Ω seems to suggest that the 'buffer' mechanism postulated above might well be responsible for the all-orders behaviour of $\mathcal{S}$. To examine this idea in more detail one can use the Monte Carlo simulation to establish whether there really is a buffer region, and to examine its size, $\eta_{\rm buffer}$, as a function of an intermediate resolution scale $t' < t$. Figure 6 shows contour plots for the distribution of $\eta_{\rm buffer}$ values as a function of t'. Here Ω is an infinite slice, and t is defined as the scale of the hardest secondary emission in Ω originating from coherent emission off partons which are to the right of Ω. Correspondingly the buffer region being considered is that to the right of Ω.

For the lower t range the buffer region tends to be fairly small — for example at $t' = 0.1$, the most likely buffer size is $\eta_{\rm buffer} \simeq 0.7$. However, increasing t to $0.55 < t < 0.65$, the most likely size of the buffer region at $t' = 0.1$ grows to $\eta_{\rm buffer} \simeq 3.5$. Such an increase in buffer size for fixed t' as one increases t is precisely what one would expect from the 'buffer' mechanism postulated earlier, eq. (4.4). From that equation one can also evaluate an effective value for $\langle \delta\eta/\delta t\rangle \simeq 9$. Using eq. (4.3), one then finds that the coefficient of t^2 in the exponent is roughly twice $\mathcal{S}_2$ for an infinite slice.

This is not quantitatively consistent with what is seen in figure 5, however several points should be borne in mind: (a) the arguments in section 4.1 are based on average properties, whereas in the end we are interested in the properties of rare events. So for example there is a certain spread in the distribution of $\eta_{\rm buffer}$ and this can affect the quantitative predictions by a non-trivial factor, as can the fact that $\delta\eta/\delta t$ is itself only defined in an average sense (b) one's estimate for $\langle \delta\eta/\delta t\rangle$ depends somewhat on how exactly one deduces it from the plots, e.g. whether as a derivative with respect to t' or t; this is connected to point (c), namely that our assumption of a constant $\langle \delta\eta/\delta t\rangle$ (independent of t') may be

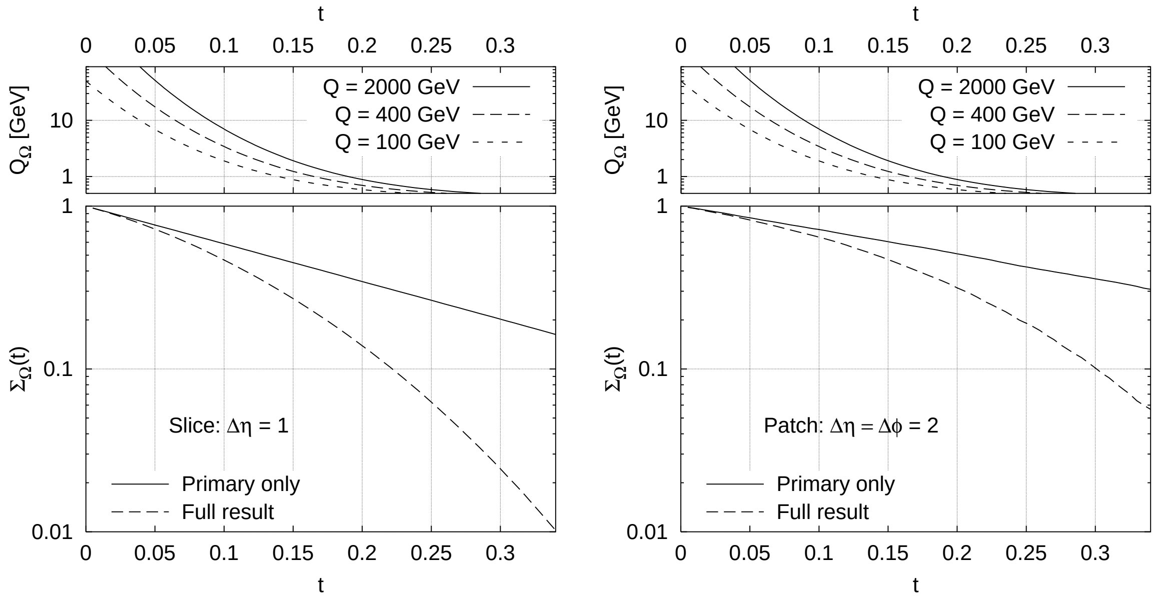

Figure 7: $\Sigma_\Omega(t)$ for two different definitions of Ω: in the left-hand figure we consider the energy flowing into a slice of width $\Delta\eta = 1$, while in the right-hand figure we consider the energy flowing into a square patch in rapidity and azimuth, of size $\Delta\eta = \Delta\phi = 2$. The upper plots show the relation between t and Q_Ω for different values of the centre-of-mass energy Q.

an oversimplification. Indeed if $\langle \delta\eta/\delta t\rangle$ is constant then, from eq. (4.4), one would expect the centre of the distribution of $\eta_{\rm buffer}$ to depend linearly on t'. However in figure 6 there seems to be some non-linear dependence of the typical $\eta_{\rm buffer}$ on t', though it is not clear whether this is an artifact of t not being sufficiently asymptotic, or whether there is extra dynamics which remains to be taken into account, such as a pile-up of emissions close to the edge of the buffer. Furthermore at $t \simeq 0.5$ the behaviour of $\mathcal{S}(t)$ departs from the initial approximate Gaussian, and starts to fall much faster, also suggesting either that $t \lesssim 0.5$ is not yet asymptotic, or that $\langle \delta\eta/\delta t\rangle$ has some extra t' dependence.

In conclusion, we believe that while we may have understood some of the gross features of the dynamics involved in the all-orders behaviour of $\mathcal{S}(t)$, in particular the importance of a buffer mechanism in determining the geometry-independent large-t suppression of $\mathcal{S}(t)$, there are some significant details which remain to be understood.

4.3 Phenomenological implications

To understand the phenomenological significance of the non-global logarithms, it is interesting to compare results for $\Sigma(t(Q_\Omega, Q))$ with only primary emissions and with the full non-global treatment. This is done in figure 7 for two different geometries of Ω, a slice in rapidity and a square patch in rapidity and azimuth. The upper plots show how t is related to Q_Ω, for different values of the centre of mass energy Q. Even at a very energetic next-linear-collider, optimistically trusting the calculation down to $Q_\Omega = 0.5\,\mathrm{GeV}$ one only just goes beyond $t = 0.25$. For current energies the largest value of t that is accessible is in the range of 0.15 to 0.2. Taking $t = 0.15$ as our reference value, the inclusion of the non-global effects increases the suppression relative to that for just primary emissions such that the ratio $\ln \Sigma_\Omega / \ln \Sigma_{\Omega,\mathcal{P}}$ takes the values 1.5 and 1.65 for the patch and slice respectively. To state it a different way, ignoring non-global effects at $t = 0.15$ overestimates the cross section by between 30% (patch) and 65% (slice). At larger t values, these figures rapidly become even more dramatic.

So the non-global effects are not only important from the point of view of the formal correctness of the leading-log series, but also numerically significant.

As an aside we comment on the feature of a divergence in the distribution of Q_Ω at the Landau pole that has been observed in certain circumstances in [3, 2]. Such a behaviour arises when the suppression from $\Sigma_{\Omega,\mathcal{P}}(t)$ is not sufficient to compensate the divergence in dt/dQ_Ω, i.e. when $C_F \mathcal{A}_\Omega / \pi\beta_0 < 1$. However the inclusion of the non-global factor $S(t)$ ensures that $\Sigma_\Omega(t)$ always goes to zero much faster than dt/dQ_Ω diverges. Therefore the distribution of Q_Ω should go to zero at the Landau pole regardless of the size of $C_F \mathcal{A}_\Omega / \pi\beta_0$.

Finally, we note that for a comparison to data it would also be necessary to take into account non-perturbative effects. One way of doing so might be in terms of power corrections [13]. For the mean Q_Ω, in a normalisation in which the power correction to the e^+e^- thrust has a coefficient $c_\tau = 2$, the coefficient for a region Ω would be $c_\Omega = \mathcal{A}_\Omega Q$ where $\mathcal{A}_\Omega$ is the area of Ω. For the corresponding differential distribution one should roughly expect a shift of the distribution by the same amount.

5. Conclusions

As has already been pointed out in [6], in the resummation of any observable which only receives a contribution from emissions in a limited angular region Ω of phase space, there is a class of single-logs — 'non-global logs' — which leads to a breakdown of the picture of independent primary emissions and strict angular ordering. That picture has been quite widely adopted in the literature, in certain instances wrongly [7, 8, 9, 3, 2, 4], at least to the accuracy that was claimed.[4] To deal with this class of terms it is necessary to consider emission from arbitrarily complicated ensembles of energy-ordered large-angle gluons lying outside the region of sensitivity of one's observable.

In this article we have considered non-global logarithms for observables such as the distribution of energy flow in restricted angular regions between jets. This kind of measurement was originally advocated, in [1, 2], for 2+2-jet events in hadron-hadron collisions. Here we have studied a simpler case, that of 2-jet events, in order to concentrate on the specific features of these non-global logarithms, without the difficulties that arise from the complex colour structure of four-jet systems. We also point out that experimental studies of interjet energy flows in e^+e^- and DIS, insofar as they are free from contamination by the underlying event, may provide useful complementary information to that which could be extracted in hadron-hadron colliders.

[4] There exist other cases, e.g. [14, 15], whose final results are for global variables, but where intermediate steps of the derivation make reference to non-global hemisphere-variables without the inclusion of non-global logs. It is important not to use those results outside the context of the specific derivation for which they are intended, without taking care of non-global effects as required.

JHEP03(2002)017

Our studies have led us to various conclusions. Most importantly perhaps, is that non-global effects, as well as being formally of the same order as those from primary emissions, are also numerically almost as large.

More academically, one of the interesting aspects of non-global logs that is specific to interjet energy flows, as opposed to the single-hemisphere observables studied in [6], is that they depend on the geometry of Ω, the region in which one measures the energy flow. At order α_s^2 (the first order at which these effects appear), for moderately sized patches, the magnitude of non-global effects is roughly proportional to the perimeter of the patch. In contrast, effects due to primary emissions scale as the area of the patch.

At all orders, we have only a large-N_C numerical treatment for non-global effects. Despite this it is possible to obtain some interesting insights into the mechanisms that are of relevance. One notable result is that, modulo a geometry-dependent normalisation, the asymptotic t-dependence of the non-global suppression factor $\mathcal{S}$ seems to be independent of the size and shape of Ω. This fact, together with figure 6, lends support to the hypothesis that at intermediate scales there is an empty 'buffer region' around Ω and that a significant part of the non-global suppression factor $\mathcal{S}$ stems from the suppression of intermediate-scale primary radiation in the buffer region. This allows us to postulate that in other processes, such as $2+2$-jet production at hadron colliders, one will see similar results, with the asymptotic t-dependence of $\mathcal{S}$ being given by that of figure 5a, raised to a power which depends on the number of jets and whether they are quark or gluon jets.

Acknowledgments

We wish to thank Yuri Dokshitzer, George Sterman and Bryan Webber for helpful discussions. One of us (MD) gratefully acknowledges the hospitality of the LPTHE where part of this work was carried out.

References

[1] G. Marchesini and B.R. Webber, *Associated transverse energy in hadronic jet production*, *Phys. Rev.* **D 38** (1988) 3419.

[2] C.F. Berger, T. Kúcs and G. Sterman, *Energy flow in interjet radiation*, hep-ph/0110004.

[3] G. Oderda and G. Sterman, *Energy and color flow in dijet rapidity gaps*, *Phys. Rev. Lett.* **81** (1998) 3591 [hep-ph/9806530].

[4] G. Oderda, *Dijet rapidity gaps in photoproduction from perturbative QCD*, *Phys. Rev.* **D 61** (2000) 014004 [hep-ph/9903240].

[5] N. Kidonakis, G. Oderda and G. Sterman, *Evolution of color exchange in QCD hard scattering*, *Nucl. Phys.* **B 531** (1998) 365 [hep-ph/9803241].

[6] M. Dasgupta and G.P. Salam, *Resummation of non-global QCD observables*, *Phys. Lett.* **B 512** (2001) 323 [hep-ph/0104277].

[7] V. Antonelli, M. Dasgupta and G.P. Salam, *Resummation of thrust distributions in dis*, *J. High Energy Phys.* **02** (2000) 001 [hep-ph/9912488]. Our comments apply only to the

JHEP03(2002)017

calculation for the τ_{zE} variable, which suffers from the problem that it is discontinuously global.

[8] S.J. Burby and E.W.N. Glover, *Resumming the light hemisphere mass and narrow jet broadening distributions in e^+e^- annihilation*, *J. High Energy Phys.* **04** (2001) 029 [hep-ph/0101226]. Our comments apply only to version 1 on the hep-ph archive, as it is only that version which makes any claims about single-log accuracy.

[9] A. Banfi, G. Marchesini, Y.L. Dokshitzer and G. Zanderighi, *QCD analysis of near-to-planar 3-jet events*, *J. High Energy Phys.* **07** (2000) 002 [hep-ph/0004027]. Our comments apply only to the calculation for the right-hemisphere $K_{\rm out}$ distribution.

[10] Y.L. Dokshitzer, G. Marchesini and G. Oriani, *Measuring color flows in hard processes: beyond leading order*, *Nucl. Phys.* **B 387** (1992) 675.

[11] A. Bassetto, M. Ciafaloni and G. Marchesini, *Jet structure and infrared sensitive quantities in perturbative QCD*, *Phys. Rept.* **100** (1983) 201.

[12] L. Lönnblad, *ARIADNE version 4: a program for simulation of QCD cascades implementing the color dipole model*, *Comput. Phys. Commun.* **71** (1992) 15.

[13] See for example Y.L. Dokshitzer, A. Lucenti, G. Marchesini and G.P. Salam, *Universality of 1/q corrections to jet-shape observables rescued*, *Nucl. Phys.* **B 511** (1998) 396 [hep-ph/9707532], erratum *ibid.* **B 593** (1998) 729 and references therein.

[14] S. Catani, L. Trentadue, G. Turnock and B.R. Webber, *Resummation of large logarithms in e^+e^- event shape distributions*, *Nucl. Phys.* **B 407** (1993) 3.

[15] Y.L. Dokshitzer, A. Lucenti, G. Marchesini and G.P. Salam, *On the QCD analysis of jet broadening*, *J. High Energy Phys.* **01** (1998) 011 [hep-ph/9801324].

JHEP03(2002)017